Zeitschrift für Physikalische Chemie, Bd. 201, S. 99–109 (1997)

Rôle of the Jahn-Teller Coupling in the Luminescence Spectra of Fe^{2+} in Zinc-Blende Compounds*

By E. E. Vogel, O. Mualin

Departamento de Física, Universidad de La Frontera, RCH-Temuco, Chile

H.-J. Schulz and M. Thiede

Fritz-Haber-Institut der MPG, Faradayweg 4–6, D-14195 Berlin, FRG

(Received August 24, 1996)

Crystal-field splitting / Jahn-Teller effect / Photo-luminescence / Self-inversion of spectral lines / Vibronic energy levels

The luminescence spectra of Fe^{2+} in zinc-blende-type II–VI and III–V compounds do not show an equally spaced set of emission lines as predicted by spin-orbit interaction in a plain crystalline field. The unequal separation between these lines is a signature of the Jahn-Teller effect in these systems. Attention is focused here on the general trend of the ^{5}E-derived energy levels providing the end states for the emission transitions. The intervall between the second and third energy levels (γ_4 and γ_3) is employed as a sensitive test based on the two following characteristics: First, this is the spacing that varies the most; second, the emissions to these levels are usually quite sharp as they involve energies not overlapping with phonon-assisted transitions. This property is studied in the plane [$\hbar\omega$,E_{JT}] (energy of the coupling phonon and the Jahn-Teller energy which is directly related to the coupling strength). The general behaviour is then studied under different theoretical conditions, in particular those that maximize the effect. Application of this theory to each real compound is thus possible by choosing the right combination of the two variables. To this end, the examples of luminescent substitutional Fe^{2+} ions in ZnS, ZnTe, and CdTe are discussed based on published spectra. The main emphasis is placed on new precise measurements of the ZnSe:Fe^{2+} emission. With crystals containing different iron concentrations, changing line shapes, including self-inversion of several emission lines, have been obtained in the 2600 to 2800 cm^{-1} spectral range. The properties of the four host/impurity systems are satisfactorily explained while an overall description emerges for the whole family of these compounds from a compilation of the derived coupling parameters.

I. Introduction

Iron enters in its doubly ionized state as a substitutional impurity in II–VI compounds with zinc-blende structure. The ^{5}D atomic manifold is split into

* Presented at the 13th International Symposium on Electrons and Vibrations in Solids and Finite Systems (Jahn-Teller Effect) Berlin 1996.

a ground ^5E and an excited $^5T_2$ multiplet by the action of the crystalline field. Spin-orbit interaction leads to a further splitting of all multiplets. The upper one leaves a triplet of symmetry T_2 (Γ_5) at the lowest energy within these excited levels. Any of these three states will act as an initial state for low-temperature emissions originating from the upper multiplet. On the other hand, the lower multiplet ^5E is left with an A_1 (γ_1) singlet as the true ground state; then going up in energy we find the electronic levels T_1 (γ_4), E (γ_3), T_2 (γ_5), and A_2 (γ_2) [1]. A level-scheme is presented in Fig. 1 of Ref. [1].

The admixture of upper atomic levels, even to a weak extent, allows electric-dipole (T_2) emissions to the levels γ_1, γ_4, γ_3, and γ_5. These are the main four lines in the spectra and will be referred to as L1, L2, L3, and L4, respectively. The second of these transitions (L2) leads to the most intense line. Plain crystal-field theory predicts four equally spaced lines in the luminescence spectra. However this is not so. The energy difference between the γ_3 and γ_4 levels (Δ_{34} from now on) is clearly smaller than expected. A different way of expressing this observation is that L2 and L3 are closer than any other pair of these main lines. Additionally, a broad structure is observed at energies lower than the transition to the γ_5 level.

All these features have been explained previously as a manifestation of a weak Jahn-Teller effect. In the present paper we investigate two aspects of this phenomenon. First, we do complete calculations to find out which is the most significant parameter for the large deviation of Δ_{34} in the systems under consideration. Second, we report new measurements to amend the picture for the cases of $ZnS:Fe^{2+}$ and $ZnSe:Fe^{2+}$.

The emission of substitutional $Fe^{2+}(3d^6)$ ions in ZnS was early detected [2] and subsequently described in a dynamic Jahn-Teller model [3]. Ensuing papers [4, 5] included spectra with higher resolution. While the cubic host materials CdTe [1] and ZnTe [6] were recently subject of combined experimental and theoretical efforts, the early report [7] on the luminescence of $ZnSe:Fe^{2+}$ did not find much extension, except for some special aspects [5]. This deficiency provided the incentive for the present study.

The just mentioned spectra are reported in the next Section. Then in Section III the results of diagonalizing the general Hamiltonian are reported, including a linear Jahn-Teller component. In Section IV we analyze this phenomenon, explain the two measured spectra, compare to the case of III−V systems, and discuss a possible extension of this treatment to other cases.

II. Experimental

Most of the ZnSe crystals used in the present investigations were grown by an iodine-transport technique in the Technical University of Berlin, some

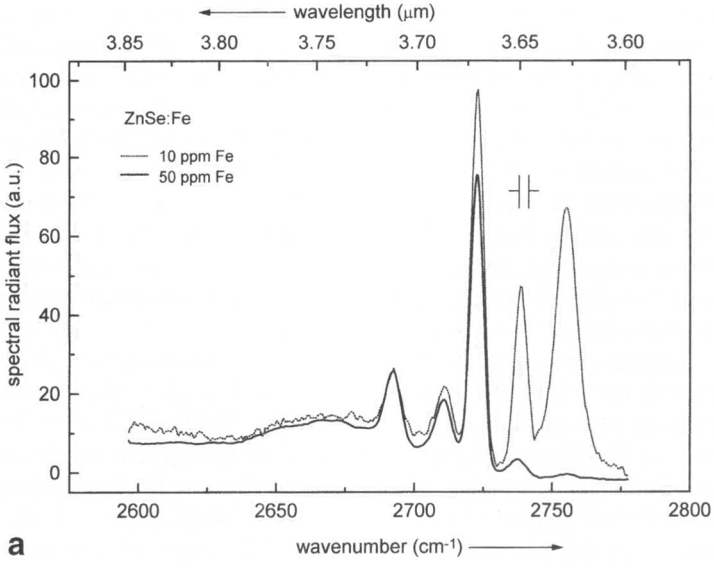

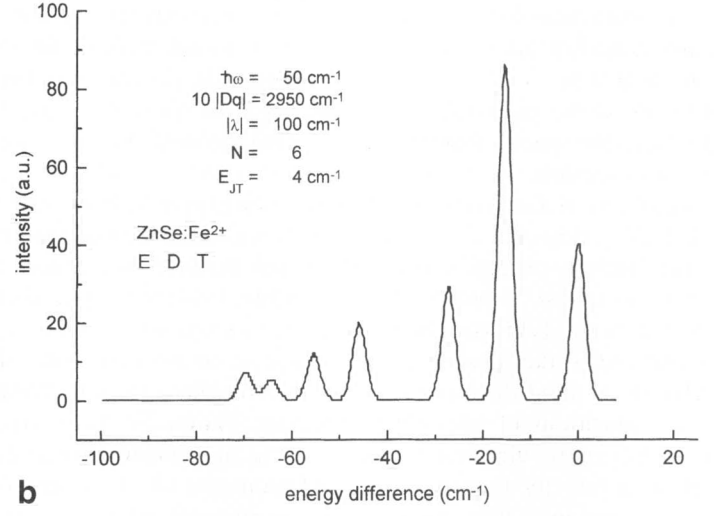

Fig. 1. a) Emission spectrum of the $^5T_2(D) \rightarrow {}^5E(D)$ transitions of $ZnSe:Fe^{2+}$ in the low-concentration limit. T = 4 K. Ar-laser excitation at 19436 cm^{-1}, crystal 5045 (10 ppm Fe nominal doping) with 1 W power, crystal 5046 (50 ppm nom.) with 0.6 W power. The line at 2755 cm^{-1} is probably caused by the presence of Fe/Ni associates. b) Theoretical spectrum for the low-temperature $^5T_2(D) \rightarrow {}^5E(D)$ emissions using a Gaussian line-shape centered at the calculated energies of the vibronic levels. Values of the parameters are given in the insert.

others obtained from a commercial source were probably melt-grown. Where a Fe content is given, the number refers to the respective amount of the dopant added to the starting material before growth and thus represents an upper limit rather than a true measure of the iron concentration. The color of the specimens varies between yellow at low Fe content and orange-brown at the highest doping levels.

The photo-luminescence experiments were normally carried out in a standard setup with either laser or xenon-lamp excitation, crystal cooling in an immersion cryostat, and lock-in technique for light detection behind an evacuable 1-m grating spectrometer. In some cases, a Fourier-transform instrument was utilized for supplementary studies.

The luminescence spectra of two ZnSe:Fe crystals with different low iron concentration levels are displayed in Fig. 1a. They show the typical fingerprint of four narrow lines, L1 to L4, at 2738.5, 2722.5, 2710.5 and 2692 cm^{-1}, L2 being the strongest transition. In the adjacent region between 2670 and 2640 cm^{-1}, a broad hill is present, while on the high-energy side a satellite line of considerable strength appears at 2755 cm^{-1}, being more pronounced for the lower-doped specimen. The origin of this line is not clear, although it had been earlier detected in ZnSe:Ni crystals [8]. A complex defect involving an iron-nickel associated center had been suggested as a possible source but this hypothesis still requires experimental confirmation. Another noteworthy feature of these Fe^{2+} spectra is the strong quenching of the line L1 for the higher doped material. This is the result of self-absorption at this line, as will be substantiated by the transmission spectra and those of the emission at even higher iron concentrations. Fig. 1b corresponds to the spectra that emerge from the theoretical calculations presented in next section.

The emission of a strongly-doped crystal (1000 ppm Fe nominal) exhibits a fairly deviating shape in the region of the main transitions (Fig. 2). While L1 is entirely absent, line L2 which was dominating the spectrum at low-doped specimens, is just barely discernible, L3 (now peaking at 2712 and 2705 cm^{-1}) and L4 (2694 and 2690.5 cm^{-1}) are split in an unsymmetrical fashion, and in the aforementioned range of an unstructured emission near 2670 cm^{-1}, three distinct peaks occur at 2682, 2674 and 2667 cm^{-1} with some indications of additional shoulders. These new structures point towards an advanced vibrational interaction in higher-doped crystals, perhaps due to a heavily perturbed local environment of the impurity. The increased absorption in this sample entails an almost total disappearance of L1 and L2 and causes a pronounced self-inversion at lines L3 and L4. Self-inversion is well-known to occur in plasma physics for systems where the spatial region of the emission would undergo stronger broadening influences than the region of absorption. Similar effects seem to be associated with the inhomogeneous broadening which rules the measured line widths here. The effect had been earlier observed with Fe^{2+} luminescence in ZnS [4].

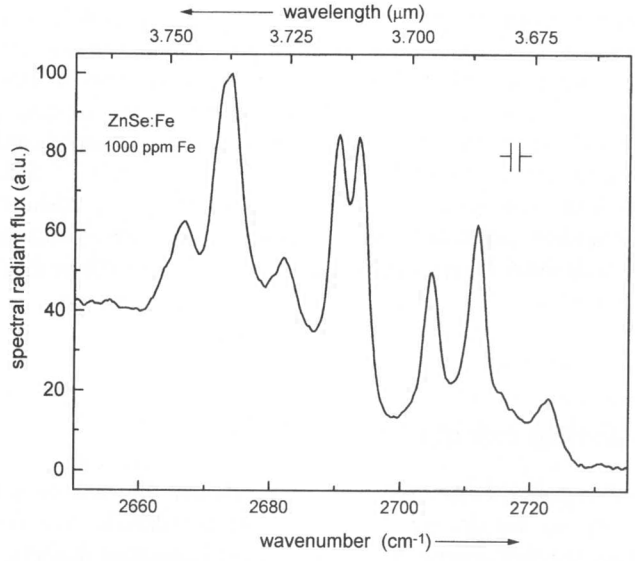

Fig. 2. Emission spectrum of the $^5T_2(D) \rightarrow {}^5E(D)$ transitions of $ZnSe:Fe^{2+}$ in the high-concentration limit. T = 4 K. Excitation: 19436 cm^{-1}. Crystal 5047 (1000 ppm nominal Fe concentration).

As an example of a transmission measurement, a spectrum taken with a nominally undoped sample in the range of the no-phonon transitions is given (Fig. 3). The lines L1 and L2 are clearly dominating here at both temperatures chosen. They experience some broadening in the T = 20 K scan. This influence leads to a blurring of L3 which is also present in both spectra. Line L4, on the other hand, is only visible in the spectrum at elevated temperature since its occurrence rests to a stronger extent than that of L3 and L2 on population of a higher spin-orbit component of the $^5E(D)$ ground state multiplet. Note that this transmission spectrum does not feature a structure attributable to the 2755 cm^{-1} line displayed by many of the Fe-doped specimens.

The self-absorption demonstrated with high Fe concentrations at lines L1 and L2 in these crystals does not only depend on the amount of iron present in a particular sample but on the excitation conditions as well. In an experiment (with crystal number 5048) this was demonstrated under 0.3 W excitation with two different laser wavelengths. The spectrum showed L1 clearly and L2 was still the dominating peak when 457.9 nm Ar laser irradiation (21,839 cm^{-1}) was used which favours surface-near regions of the sample, whereas on 514.5 nm excitation (19,436 cm^{-1}) which penetrates deeper into lattice, L1 is strongly quenched and L4 becomes predominant like in Fig. 2. An absorption measurement with the same sample confirmed

a transmittance of approximately 10% at the lower excitation energy whereas the specimen is nearly opaque at the higher photon energy. These findings support the assumption that the diminution of emission lines is connected with their generation in the bulk regions of the sample. The self-inversion occurring moreover in some instances could additionally be related to temperature differences between bulk and surface, so that emission originating in the volume at an elevated temperature (as a result of heating under the exciting radiation) would experience self-absorption mainly on passing through outer layers which are cooler because of their direct contact with the coolant.

III. Theoretical calculations

Calculations reported below are based on a theory that has been presented elsewhere [9], so we do not need to repeat the details. For the sake of completeness we will merely review the most important aspects, to define the scope of the treatment and the notation to be used below.

We assume that doubly degenerate phonons of symmetry ε (or γ_3) are responsible for the coupling to the electronics levels of the multiplet ^{5}E. The basis is formed in the adiabatic limit by direct products like:

$$(\varepsilon)^{\nu} \otimes (\gamma_1 + \gamma_4 + \gamma_3 + \gamma_5 + \gamma_2)\,, \tag{1}$$

with $\nu = 0, 1, 2, 3, \ldots N$, where N is a number of vibrational quanta that guarantee stability of the solutions. The resulting vibronic functions are denoted as:

$$|\tilde{\gamma}_f(\gamma_i, \nu)\rangle\,, \tag{2}$$

where γ_i corresponds to the symmetry of the initial electronic functions, ν is the number of vibrational quanta (or amplitude of the coupling phonon) and $\tilde{\gamma}_f$ represents the symmetry of the final vibronic function. Selection rules for electric-dipole transitions (EDT's) eliminate states $\tilde{\gamma}_2$ as possible end levels, while all other states with significant zero-phonon component are allowed.

The electronic problem is assumed to be solved, so parameters for crystalline field ($10|Dq|$) and spin-orbit interaction ($\lambda\ \mathbf{S}\cdot\mathbf{L}$) are known. The latter is taken with its value for the free ion, namely $\lambda = -100\ \mathrm{cm}^{-1}$; in this way the effect of the vibronic coupling reveals itself in a clearer way. The parameter $10|Dq|$ depends on the host crystal and is fixed by considering the highest-energy line, after considering corrections up to second order in the spin-orbit interaction [10]. It is found that the values for ZnS:Fe^{2+} and ZnSe:Fe^{2+} are 3158 cm^{-1} and 2944 cm^{-1}, respectively.

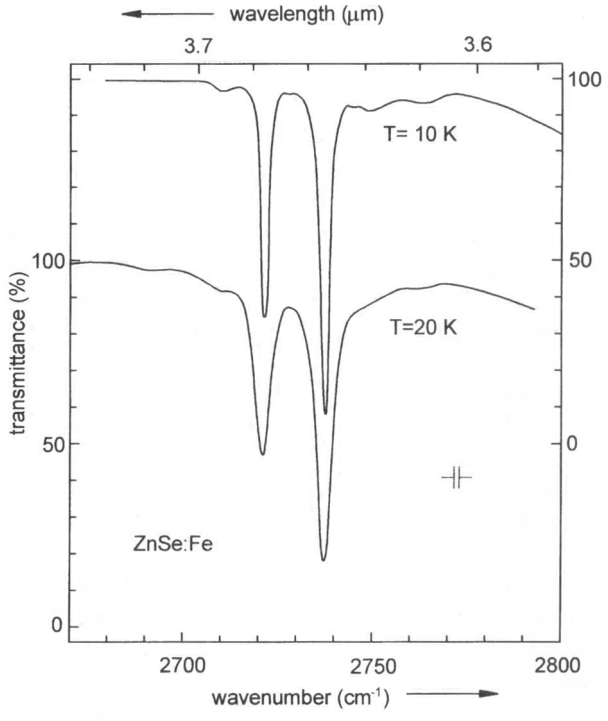

Fig. 3. Transmission spectrum in the range of the main no-phonon transitions of ZnSe:Fe^{2+} at two different temperatures. Crystal C 109, not intentionally iron doped. Note that the traces have been shifted in the vertical direction for clarity.

The vibrational Hamiltonian for the two coupling modes θ and ε of energy $\hbar\omega$ is expressed as

$$\mathcal{H}_{v} = \hbar\omega(a_\theta^\dagger a_\theta + a_\varepsilon^\dagger a_\varepsilon + 1), \tag{3}$$

where the usual creation and annihilation operators $a_\alpha^\dagger$ and a_α are used. ($\alpha = \theta, \varepsilon$).

The coupling Hamiltonian can now be written as

$$\mathcal{H}_{JT} = \sqrt{\hbar\omega\, E_{JT}}\,[(a_\theta^\dagger + a_\theta)D_\theta + (a_\varepsilon^\dagger + a_\varepsilon)D_\varepsilon], \tag{4}$$

where E_{JT} is the so-called Jahn-Teller energy and D_θ and D_ε are normalized electronic operators. In all the results reported below this is the only adjustable parameter.

We consider here coupling modes corresponding to the points TA(L) of the Brillouin zone, since they have given good results for Fe^{2+} in III–V compounds with zinc-blende structure [1, 9]. The values of $\hbar\omega$ are then obtained from the literature [11–16]: 70 cm^{-1} for ZnS and 50 cm^{-1} for ZnSe.

Diagonalizations are now performed by varying E_{JT}. Calculations are done by using group theory to sort the functions. This procedure permits to break the total Hamiltonian matrix into the submatrices allowed by the local symmetry at the site of the impurity. Good agreement with experiment is found for 6 cm^{-1} in the case of ZnS and 4 cm^{-1} in ZnSe. A finer variation of E_{JT}, although possible, did not seem to be relevant at this point.

In the spectrum of the higher doped ZnSe crystal the broad structure to the left of the four sharp lines is resolved as shown in Fig. 2. But this was already anticipated in the theoretical spectrum shown in Fig. 1b. This is a confirmation of the complete description of this emission spectrum by the method and techniques described above. The three lines at 2682, 2674, and 2667 cm^{-1} are theoretically explained within a ± 1 cm^{-1} precision.

In previous studies we had found a common value of 3 cm^{-1} for E_{JT} in the cases of ZnTe:Fe^{2+} and CdTe:Fe^{2+} [1, 6]. The complete set of results presents a homogeneous description of Fe^{2+} in the family of II–VI compounds with zinc-blende structure, with values that are slightly lower than those found for III–V compounds, where values for E_{JT} of 7 to 8 cm^{-1} were obtained [9].

To make sure that these values are suitable from the point of view of numerical analysis, N was increased in steps of unity up to a point where the eigenvalues stabilize. We use the criterion that Δ_{34} must be defined with two significant figures when increasing from $(N-1)$ to N [17].

The vibronic functions as found after agreement with experiment and stability of the numerical results can be used to calculate relative oscillator strengths (ROS) for electric-dipole transitions without any further adjustment. These relative intensities can now be used in a Gaussian line-shape analysis. In Fig. 1b we present such a result to compare with the experimental spectrum for ZnSe:Fe^{2+} shown in Fig. 1a. Similar good agreement is obtained for the emission lines of ZnS (not shown here). However, this spectrum is less interesting than the others due to the weaker manifestation of the Jahn-Teller effect, caused by a larger value of $\hbar\omega$, as follows from the discussion below.

IV. Discussion

In both compounds studied here the positions and intensities of the four distinct peaks present in the luminescence spectra are well explained by the introduction of a Jahn-Teller term. If such a coupling would not exist then the energy differences between two successive levels would be all the same, which is not so.

The most sensitive among the successive energy differences, named Δ_{34} (the energy difference between levels $|\tilde{\gamma}_4(\gamma_4,0)\rangle$ and $|\tilde{\gamma}_3(\gamma_3,0)\rangle$), is presented

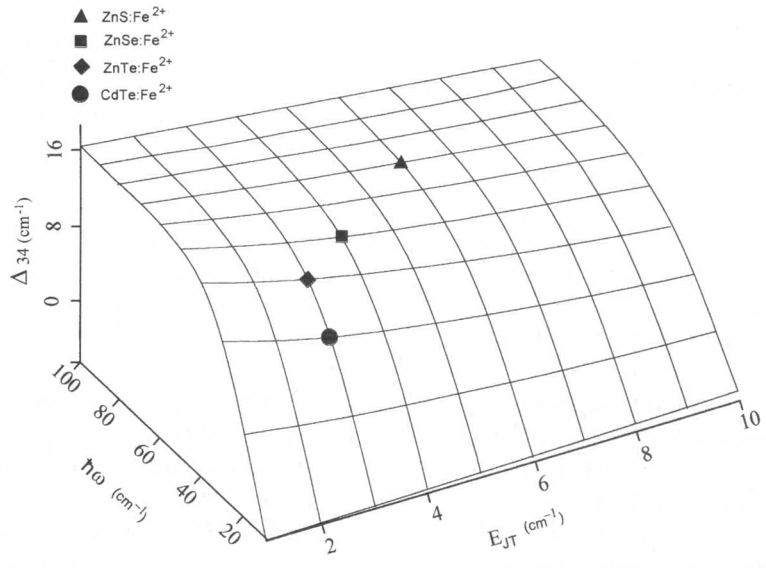

Fig. 4. Energy difference Δ_{34} between the lowest γ_3 and γ_4 vibronic levels. (It also corresponds to the energy difference between lines L3 and L2) as function of the energy of the coupling phonon ($\hbar\omega$) and the Jahn-Teller energy (E_{JT}). The crystal-field parameter corresponds to ZnSe:Fe^{2+} but the four systems are included under the same description since only very small differences are produced by the individual values of the different crystalline fields.

in Fig. 4 as a mathematical function of $\hbar\omega$ and E_{JT}. The value of $10|Dq|$ used here was 2950 cm^{-1}, but the numerical results do not vary strongly with changes of this parameter.

It turns out that it is not the Jahn-Teller energy (strength of the coupling) which is the most important variable for modifications of the spectrum. It is $\hbar\omega$ that produces a strong decrease of Δ_{34} (and other intervals) as this parameter approaches particular values that are close to electronic energy differences. This shows that even in the weak-coupling limit values of $\hbar\omega$ near resonant conditions can make the Jahn-Teller effect a very important feature of such systems.

On Fig. 4 we have also marked the points close to the actual solutions of Fe^{2+} in all II−VI compounds with zinc-blende structure. Although the value of $10|Dq|$ is appropriate for ZnSe:Fe^{2+}, the main experimental trend is confirmed. Actually the case of ZnS:Fe^{2+} exhibits the most regular spectrum while CdTe:Fe^{2+} reported earlier [1], presents the most irregular distribution of vibronic energy levels with the smallest separation Δ_{34}.

Beyond the four leading lines L1, L2, L3, and L4, we also resolved and explained theoretically the three additional lines towards the low-energy side of the spectrum. They are weak lines originating from the small zero-

Table 1. Résumé of parameters of crystalline field ($10|Dq|$), energy of the coupling phonon ($\hbar\omega$), and Jahn-Teller energy (E_{JT}) used in the best adjustment of luminescence spectra of the systems indicated in the first column. All energies in cm^{-1}. (ZnS: present paper; ZnSe: present paper; ZnTe: Ref. [6]; CdTe: Ref. [1]).

System	$10\|Dq\|$	$\hbar\omega$	E_{JT}
ZnS : Fe^{2+}	3158	70	6
ZnSe : Fe^{2+}	2950	50	4
ZnTe : Fe^{2+}	2692	40	3
CdTe : Fe^{2+}	2470	30	3

phonon component present in states where the one-phonon component dominates. In the heavily doped samples these transitions are emphasized due to the diminished intensities of the main lines because of self-absorption, a process that is less likely for one-phonon states.

At this point, it is interesting to gather in Table 1 all the parameters used in these adjustments combining the two compounds reported here plus the other two compounds previously reported.

Stability of the numerical solutions was also investigated using the values of the parameters reported in Table 1. The results for Δ_{34} in the four systems stabilize at $N=3$ already. Nevertheless, all calculations presented here were done up to $N=6$ for even higher precision.

V. Concluding remarks

The general characteristics of the spectra of Fe^{2+} in II–VI and III–V compounds with zinc-blende structure is also observed in the systems ZnS:Fe^{2+} and ZnSe:Fe^{2+}: four lines almost equally spaced (the second being the most intense one), followed by some irregular broad structure towards lower energies. The energy difference between successive levels is more regular for ZnS than for ZnSe. By the same token, the additional lower-energy broad structure is better discernible for ZnSe than for ZnS.

The spectra presented above clearly establish the phenomenon of self-absorption in these systems. This is more notorious for the heavily doped samples as well as when a more penetrating source of excitation is used.

The main features of the spectra, such as energy of the lines and relative intensities of the emissions, are well explained by the introduction of a linear Jahn-Teller Hamiltonian based on the coupling to a doubly degenerate phonon group, corresponding to the TA(L) points of the Brillouin zone possessing ε symmetry. Thus $\hbar\omega$ is taken from the lattice dynamics without further variations. The values of E_{JT} and $\hbar\omega$ are reported in Table 1.

Diagonalization in the plane $(\hbar\omega, E_{JT})$ is an interesting mathematical exercise which shows that the final spectrum is more sensitive to resonant values of $\hbar\omega$, than to a high value of E_{JT}.

Acknowledgements

We are indebted to J. Broschat, Technical University of Berlin, for growing some of the ZnSe samples employed here and to Dr. G. Roussos for performing some of the initial measurements on these. We thank Kernforschungszentrum (Karlsruhe, Germany) and Fundación Andes/Conicyt (Chile) for partial support. The first two authors also acknowledge FONDECYT (Chile) under Grant 1960972 and Dirección de Investigación y Desarrollo of Universidad de La Frontera for partial support.

References

1. E. E. Vogel, O. Mualin, M. A. de Orúe, J. Rivera-Iratchet, M. L. Flores, U. W. Pohl, H.-J. Schulz and M. Thiede, Phys. Rev. B **50** (1994) 5231.
2. G. A. Slack and B. M. O'Meara, Phys. Rev. **163** (1967) 335.
3. F. S. Ham and G. A. Slack, Phys. Rev. B **4** (1971) 777.
4. G. Grebe and H.-J. Schulz, Z. Naturforsch. **29a** (1974) 1803.
5. G. Roussos, H.-J. Schulz and M. Thiede, J. Lumin. **31/32** (1984) 409.
6. H.-J. Schulz, M. Thiede, U. W. Pohl, J. Rivera-Iratchet, M. A. de Orúe, M. L. Flores, O. Mualin and E. E. Vogel, Z. Phys. B **98** (1995) 215.
7. J. H. Haanstra, Proc. Int. Conf. II–VI Semiconducting Compounds 1967 (D. G. Thomas, ed.) New York: Benjamin (1967) p. 207.
8. G. Roussos, J. Nagel and H.-J. Schulz, Z. Phys. B **53** (1983) 95.
9. E. E. Vogel, O. Mualin, M. de Orúe and J. Rivera-Iratchet, Phys. Rev. B **44** (1991) 1579.
10. J. Rivera-Iratchet, M. A. de Orúe, M. L. Flores and E. E. Vogel, Phys. Rev. B **47** (1993) 10164.
11. N. Vagelatos, D. Wehe and J. King, J. Chem. Phys. **60** (1974) 3613.
12. C. Patel, W. F. Sherman and G. R. Wilkinson, J. Mol. Struct. **79** (1982) 297.
13. T. Soma and H.-Matsuo Kagaya, Solid State Commun. **46** (1983) 885.
14. H.-Matsuo Kagaya and T. Soma, Phys. Status Solidi (b) **121** (1984) K 113.
15. H.-Matsuo Kagaya and T. Soma, Phys. Status Solidi (b) **124** (1984) 37.
16. B. Hennion, F. Moussa, G. Pepy and K. Kunc, Phys. Lett. A **36** (1971) 376.
17. E. E. Vogel, J. Rivera-Iratchet and M. A. de Orúe, Phys. Rev. B **38** (1988) 3556.